



Investigation of die designs on welding quality and billet material utilisation for multi-container extrusion of wide stiffened aluminium panels

Zhe Zhang¹ · Wenbin Zhou² · Zhusheng Shi¹ · Jianguo Lin¹

Received: 13 January 2023 / Accepted: 9 June 2023 / Published online: 23 June 2023
© The Author(s) 2023

Abstract

Wide stiffened aluminium panels are extensively used in aerospace, marine, and civil industries due to their light-weight structure and high stiffness. In this paper, a wide stiffened aluminium panel was manufactured using the principle of the multi-container extrusion, and a comparative study was conducted using two different die designs at the same extrusion condition, in which metal flow behaviour, extrusion force, welding quality, and billet material utilisation have been investigated numerically. Additionally, the effect of extrusion speed on the extrusion process was evaluated with the modified design. It was shown that, compared with the initial design, better metal flow behaviour can be obtained in the modified design. Multi-container extrusion greatly reduces the extrusion force, and the modified design results in a more uniform extrusion force for each extrusion container. The total extrusion force for the modified design is slightly higher compared with the initial die design, due to the increased friction in the upper die channels and the second-step welding chamber. Besides, the modified design of the multi-container extrusion can obtain better welding quality evaluated by different welding criteria, and the extrusion speed has a minor effect on the welding quality. The most notable feature is that the modified design greatly improves the material utilisation, which could save 39.5% material compared to the initial design.

Keywords Multi-container extrusion · Die design · Wide stiffened aluminium panels · Extrusion force · Extrusion welding · Material waste

1 Introduction

With the increasing demand for energy saving and CO₂ emission reduction, wide stiffened aluminium panels, which can greatly reduce the weight of structural components and improve stiffness, have received more and more attention worldwide [1, 2]. They have been widely applied in many industrial fields, including aerospace applications of aircraft wings and fuselage assembly, ship structures such as deck and hull, building constructions of blast walls, and slab-girder bridges. [3, 4]. However, manufacturing wide

stiffened aluminium panels is still a challenge in industries due to the structural complexity.

Compared with some manufacturing methods of stiffened panels such as riveting [5], welding [6], and machining [7], extrusion has the advantages of achieving good mechanical properties and high efficiency of mass production. Besides, it enables to produce integral profiles with good structure integrity and light-weighting features, which can significantly cut the cost [8]. However, the main difficulty of using extrusion to produce wide stiffened panels is that the extrusion force is high and the width of extrudates is limited by the dimensions of extrusion containers and extrusion capacity [9]. Generally, to reduce extrusion force, stiffened panels can be extruded by using flat containers/billets, but the life of the flat extrusion container is relatively short [10]. Spread extrusion has been developed to widen the width of extrudates. Liu et al. [11] produced an AA6061 aluminium stiffened plate with a width of 262.6 mm and a wall thickness of 14.14 mm by using spread extrusion. But it is difficult to produce thin-walled profiles with a large extrusion ratio. Some researchers

✉ Wenbin Zhou
wzhou001@dundee.ac.uk

¹ Department of Mechanical Engineering, Imperial College London, South Kensington Campus, London SW7 2AZ, UK

² School of Science and Engineering, University of Dundee, Dundee DD1 4HN, UK

obtain wide stiffened panels by welding extruded profiles. Aalberg et al. [12] produced a 1.26-m wide panel, built with extruded L-shaped AA6082 aluminium profile with a width of 252.5 mm, joined together by welding. Valente et al. [13] utilised the friction-stir welding (FSW) to assemble several extruded stiffened panels to widen the width. Within the extruded sections, a heat-affected zone (HAZ) would be in the vicinity of the welding lines between stiffeners on the plate, where residual stress is created. Therefore, extruding wide integral stiffened aluminium panels is increasingly concerned in recent years. NASA 'Integral Airframe Structures' program [14] proposed a method of postproduction flattening after extrusion to widen the width of extruded stiffened profiles. V-, U-, C-, and O-shaped extruded stiffened panels would be flattened and rolled to obtain the wide plates with stiffeners in this program. Although the extrusion process is similar to the traditional extrusion, the subsequent operations are complicated, as the equipment improvement would be required to grab, stretch, flatten, and roll the extruded profiles. Therefore, it is necessary to develop a novel extrusion technique to produce wide aluminium stiffened panels with low extrusion force.

It is known that extrusion force can generally be reduced by reducing the extrusion ratio. Recently, multi-container extrusion technique was proposed, which can greatly reduce the extrusion force and widen the width of profiles effectively [15, 16]. The principle of using the multi-container extrusion to reduce the extrusion force is that multiple billets are extruded into channels of the upper die, then welded together in the welding chamber, and finally form integral large panels with stiffeners. By using several small-diameter billets rather than a large-diameter billet, the extrusion ratio can be greatly reduced. Therefore, the extrusion force decreases with increasing number of containers. However, in their study [15, 16], the issue of billet material waste in the upper and lower die structures of the multi-container extrusion system is evident and needs to be minimised.

The extrusion die is crucial in the multi-container extrusion, affecting material flow and extrudate quality. A well-designed die ensures uniform velocity distribution, preventing defects and maintaining microstructure uniformity [17]. Designing a die requires an understanding of metal flow, velocity and temperature fields, and stress and strain distribution, but obtaining this information is complex. Traditionally, die design relies mostly on experience, leading to costly modifications during production [18]. Nowadays, numerical simulation is commonly used to predict the deformation of materials in the extrusion process to satisfy short-cycle production and low cost [19, 20]. The defects in the practical extrusion process could be predicted and thus allowing the initial design to be corrected prior to fabrication, which has been a trend in the modern extrusion industry. Many researchers have carried out finite element (FE) simulation

work on the extrusion die designs of aluminium profiles. Zhou et al. [21] compared the properties of wide thin-ribbed Z-shaped aluminium profiles formed using sideways and forward extrusion dies in actual extrusion and FE modelling, and they used FE simulation to describe the deformation mechanisms in actual extrusion. Chen et al. [22] analysed the porthole extrusion die design of a hollow, thin-walled aluminium profile by means of numerical simulation based on the arbitrary Lagrangian–Eulerian (ALE) method, and a design route for controlling the metal flow uniformity at the die bearing was proposed. Liu et al. [23] numerically and experimentally studied the extrusion die optimisation for a large, multi-cavity A6005 aluminium profile used on high-speed trains, and an optimised die design with little exit velocity difference was obtained. In the work, FE method was used to optimise the extrusion dies and facilitate the understanding of the deformation behaviour in various extrusion processes of aluminium profiles.

In this paper, modified extrusion dies were designed for the multi-container extrusion in order to reduce material waste and improve metal flow uniformity and welding quality. A comparison of the initial die design and modified die design is presented in terms of extrusion force, velocity distribution, welding quality, die deflection, and material waste. Besides, the extrusion force and material utilisation of the traditional extrusion and the multi-container extrusion were also compared. The defects existing in the initial die design were identified. The material flow behaviour was investigated by analysing the simulated results, and the effect of extrusion speed on the welding quality in the multi-container extrusion was studied. This work provides references for the design of extrusion dies for wide stiffened aluminium panels formed by the multi-container extrusion.

2 Die designs of multi-container extrusion

2.1 The profile

The cross-section shape and dimensions of the stiffened aluminium panel in this study are shown in Fig. 1. This profile is composed of six ribs and a base plate with a symmetric shape. The width of the base plate is 177 mm, and the thickness is 3 mm. The height and width of the ribs are 12 and 2.5 mm, respectively, and the gap between neighbouring ribs is 27 mm. The cross-section area of the profile is 711 mm², with a width-to-thickness ratio of up to 59, which makes it difficult to be extruded by conventional methods.

2.2 The initial extrusion die structure (design 1)

The dies for the multi-container extrusion generally consist of two parts, namely, the upper die and the lower die.

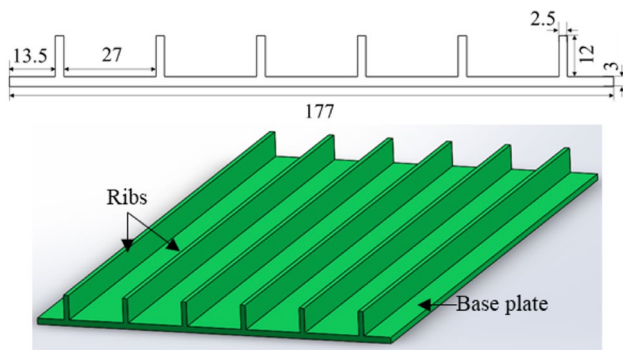


Fig. 1 Geometry and dimensions of the stiffened aluminium alloy panels to be extruded (units: mm)

Figure 2 shows the initial die design (termed design 1 afterwards) used in this study, which was slightly altered from the design in the previous study [16] by changing the flat plate outlet in the lower die to a ribbed plate outlet. There are three containers with 37 mm diameter in the extrusion container, and the gap between neighbouring containers is 22 mm. The width and height of the extrusion container and both dies are 350 mm and 230 mm. The thickness of the upper die is 50 mm. Channels in the upper die are spreading structures, as can be seen in Fig. 2b. The height and overall width of the channel outlet are 38 mm and 220 mm, which

are the same as that of the welding chamber in the lower die. The depth of the welding chamber is 15 mm. The disadvantage of this die design is that a great deal of material is wasted due to the relatively large channels and welding chamber; hence, it is necessary to improve the die structure of the multi-container extrusion.

2.3 The modified extrusion die structure (design 2)

In order to reduce material waste, upper and lower die structures are modified, which is named design 2. The geometry and dimensions of both dies are shown in Fig. 3. The following dimensions in design 2 are kept the same as design 1: the length and width of the upper die and the lower die and the total depth of the welding chamber. However, the thickness of the upper die and the lower die, the shape of the channels, and the shape of the welding chamber are changed for optimisation. For the upper die (Fig. 3a), the thickness is reduced to 25 mm, and the height and total width of the channel outlet are decreased to 26 and 190 mm, respectively, which can greatly reduce material waste in the channels. In addition, during the metal flow process in channels, the metal flow is subjected to the force of the upper and lower channel walls, which is conducive to the expansion of the metal to both sides effectively. However, in design 1, the metal flows to both sides mainly due to upsetting. The diameter of the channel entrances is 37 mm,

Fig. 2 a–c The initial design (design 1) of multi-container extrusion (units: mm)

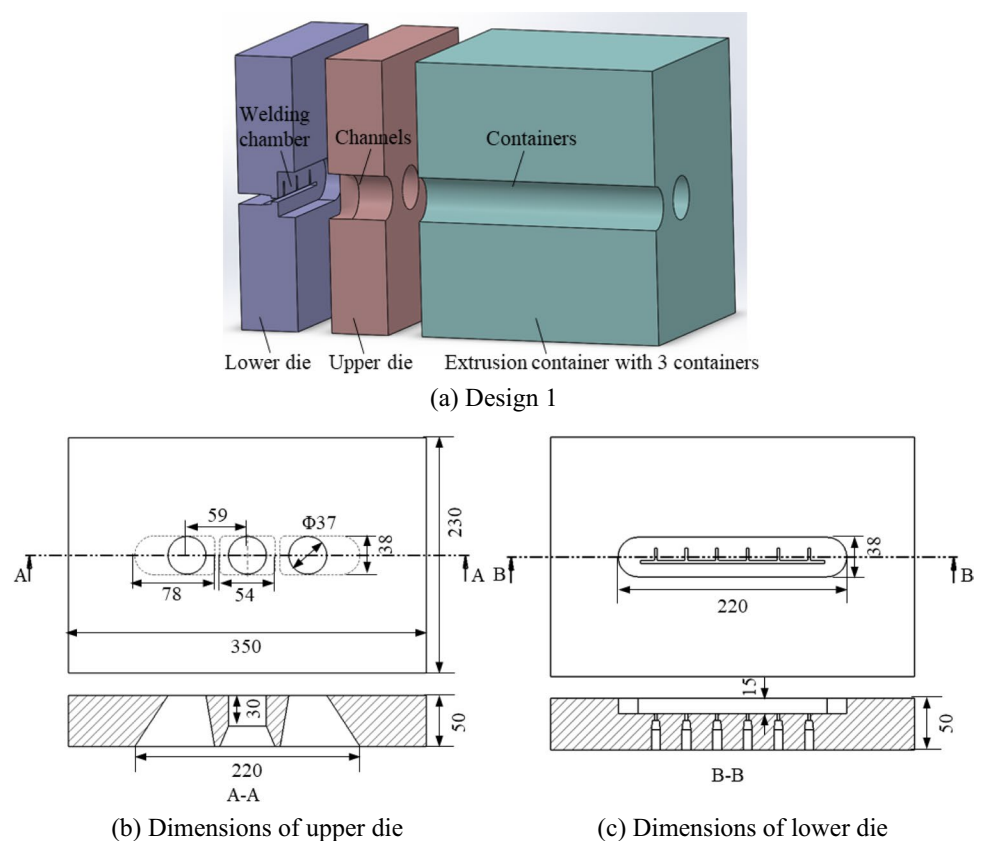
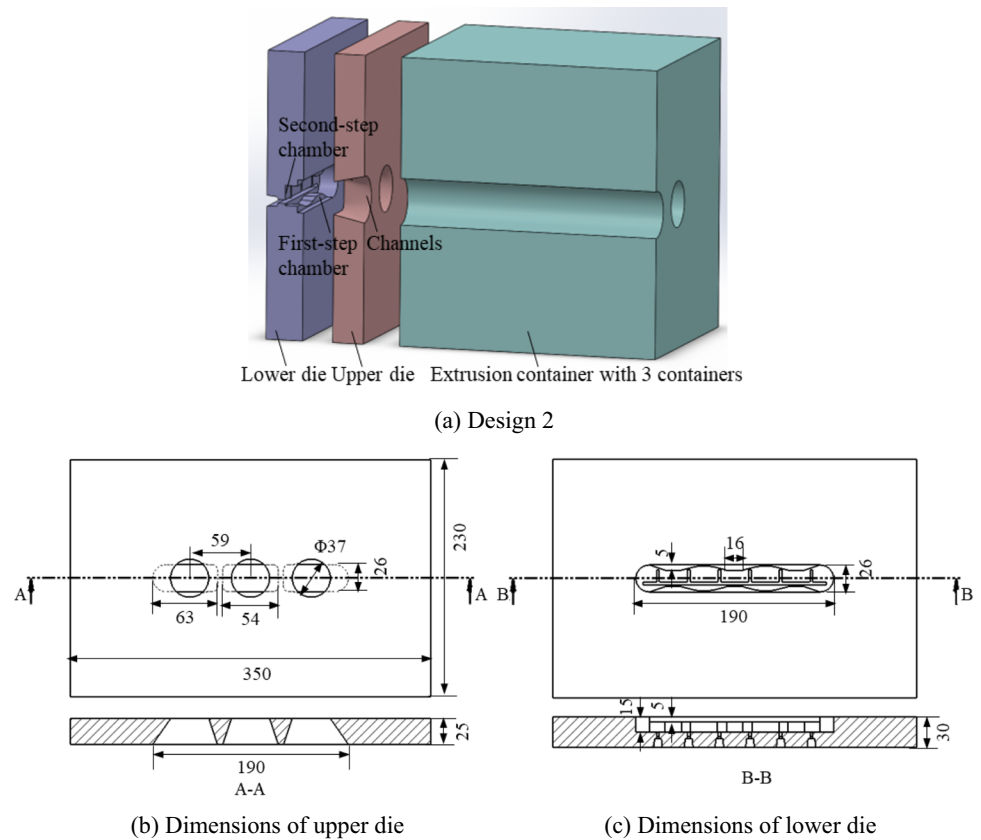


Fig. 3 a–c Geometry and dimensions of the modified die design (design 2) (units: mm)



and the gap between channels is 22 mm, the same as that of initial design 1. The outlet width of the middle channel and side channels is 54 mm and 63 mm. Figure 3c shows the modified lower die and its geometry. The dimension of the lower die is 350 mm × 230 mm × 30 mm. The welding chamber can collect materials that flow through the channels and weld the three metal flows to be an integral body. Material gradually builds up in the welding chamber, and the hydro-pressure inside the chamber increases until the material flows out of the die orifice. The welding chamber structure is critical to the quality of extrudates, and a second-step welding chamber has been proven to be effective in controlling metal flows [22, 24]. Therefore, in this case, a double-step welding chamber is introduced with a depth of 5 mm for the first-step chamber and 10 mm for the second-step chamber. The overall depth of the welding chamber is the same as that of design 1 for the purpose of comparing the welding quality of extrudates. The shape and dimensions of the double-step welding chamber are also shown in Fig. 3b. The width and height of the first-step welding chamber are 190 mm and 26 mm, respectively. The volume of the entire welding chamber of design 2 is much smaller than that of design 1, which could reduce the material waste in the welding chamber.

3 Numerical procedures

Finite element modelling was conducted using QForm-3D code to compare and understand the flow patterns and plastic deformation characteristics of the multi-container extrusion, for both design 1 and design 2 of extrusion dies. The simulation used the Lagrangian method, and the integration was explicit. Billets, container, and dies were meshed with tetrahedral elements, with finer meshes in the flange areas of die orifices. The mesh adaptation was used in workpieces and tools, in which the adaptation factor is 1 and the acceleration coefficient is 1.5. Remeshing during simulations was set with a maximum step size of 20, which means remeshing would occur when computing is up to 20 steps. The diameter of billets was 37 mm, the same as that of containers (entrance channels), and the billet length was 185 mm. The material of billets was AA6063 and that of extrusion tooling was H13. The material properties used in the simulation were from the QForm software, including the flow stress of AA6063, density, Poisson's ratio, Young's modulus, and thermal expansion of both billet material and tooling material. For friction between workpieces and extrusion tools, the Levanov friction law was applied:

$$\tau = m \frac{\sigma}{\sqrt{3}} (1 - e^{-n \frac{\sigma_n}{\sigma}}) \tag{1}$$

where τ is the friction stress, m is the friction factor, σ is the flow stress of AA6063 alloys, σ_n is the normal contact pressure, and n is the Levanov coefficient. In this study, friction factor m was set as 1, and Levanov coefficient n was 1.25 [25]. Levanov friction law in fact is a generalisation of the Coulomb friction law ($\tau = \mu\sigma_n$) and the Siebel friction law ($\tau = m \frac{\sigma}{\sqrt{3}}$), where μ is friction coefficient. The Coulomb friction model was applied for friction between extrusion tools without lubricant, where μ is 0.3 [25]. As for friction between billets, the sticking friction law was used and set as non-separable. Heat losses due to convection and radiation in the extrusion process are defined by the heat transfer coefficient and emissivity coefficient. The coefficients of heat transfer between billet and tool, between tools, and between tool and air were set as 30,000, 3000, and 30 W/(m² · K), respectively [25]. Emissivity coefficient between tool and air was 0.6 [25]. Environment temperature was set as a constant value of 20 °C.

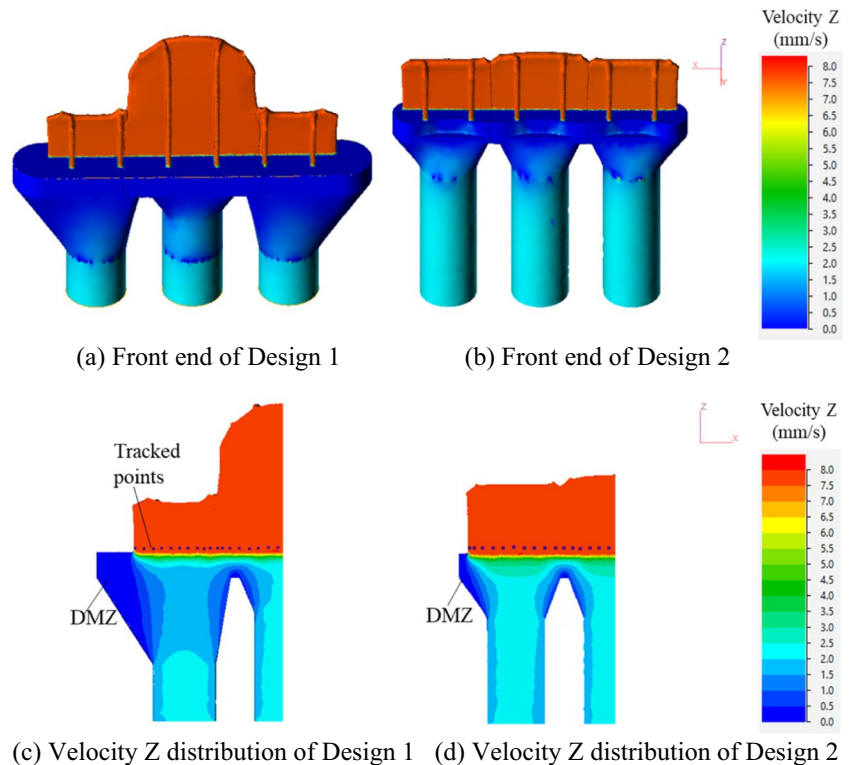
In the FE simulation of the multi-container extrusion, the initial temperatures of billets and extrusion tools were set to be 480 °C and 450 °C respectively, and the ram speed was 0.5, 1, and 2 mm/s. The extrusion ratio which was the ratio of the sum of the cross-sectional areas of the three billets to that of the product was 4.54 for the multi-container extrusion.

4 Results and discussion

4.1 Metal flow and velocity distribution

Figure 4 shows the FE results of using different extrusion dies with an extrusion speed of 2 mm/s. It shows that the front end of using modified dies is better than that of initial dies. The front end of design 2 is much flatter than that of design 1 so that less extrudate needs to be cut off. In the initial dies, the side parts take a lot of time to fill the channels and weld chambers on both sides when the middle part is extruded out, leading to a much longer middle part than others, as shown in Fig. 4a; while in the modified design, the difference in the front end is minimal among the three parts. Another obvious feature of design 1 is that most of the material is used to fill the extrusion channels, resulting in a large amount of material waste. The structure of both designs is symmetrical, so Fig. 4c, d shows a half-model. Figure 4c, d illustrates the metal flow velocity distribution of the billets during steady-state extrusion for the initial and modified designs. The results indicate that the material flow velocity at the centre of the container is higher compared to the periphery due to the friction between the workpieces and extrusion tools, which slows down the metal flow at the periphery. Figure 4c, d also shows the tracked points for the later analysis. The dead metal zones (DMZ) would be formed at the corner of the upper die and the lower die. The

Fig. 4 a–d FE simulation results for the two die designs showing the differences of the extrusion front end and velocity distribution with the same extrusion speed of 2 mm/s



material flow velocities at the sidewall and corner of the dies are almost close to zero due to the strong stick friction. It is worth noting that DMZ in design 1 is much larger than that of design 2, which means it would waste more material in this area.

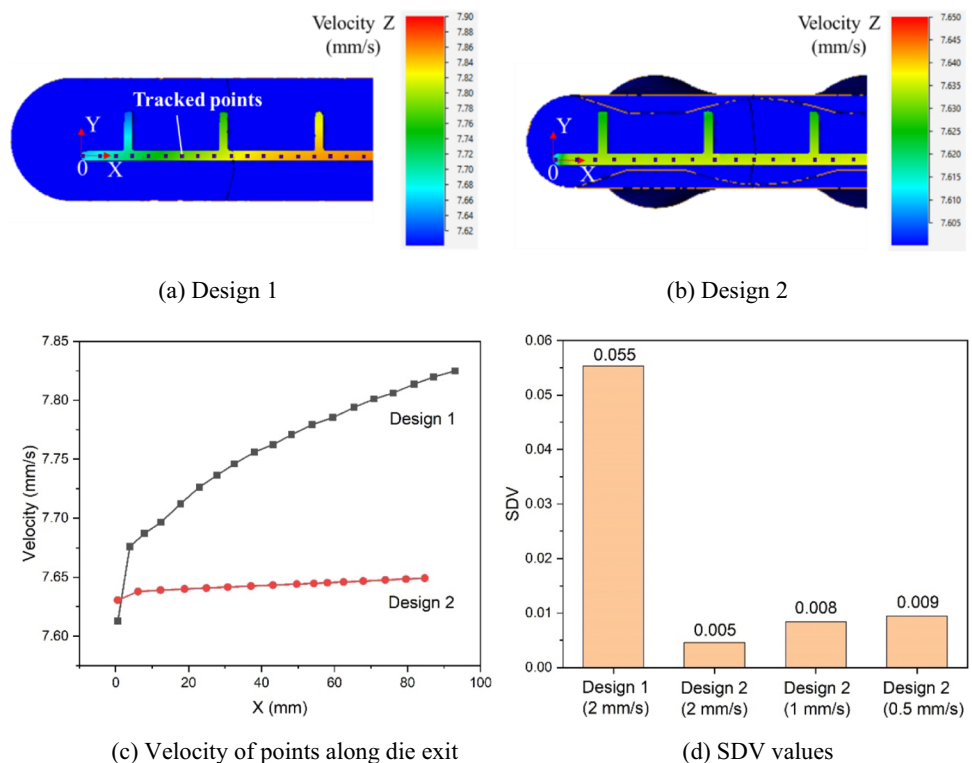
The behaviour of metal flow during extrusion is a significant factor influencing the quality of the final product. Under the condition of nonuniform metal flow, the material extruded from the die orifice has a different velocity throughout its cross-section, which easily causes the twist and bending of the products. Therefore, a uniformity of exit velocity distribution should be highly valued. In order to balance the local metal flow of the extrudate, a second-step welding chamber is adopted in the lower die and the shape of the second-step chamber also has an effect on the material flow in this study. The shape and size of the second-step chamber significantly affect the extrusion pressure, material flow, and seam quality [24]. The geometry of the second-step chamber can be modified to adjust metal flow to make the exit speed of the extrudate more uniform. However, the shape of the first-step chamber is determined by the channels, which cannot be changed at random. Figure 5a, b shows the velocity distribution of the extrudate at the exit of the extrusion die. For both dies, the velocity in the middle part of the stiffened panel is faster than that of the side parts, and the velocity of the plate part is faster than that of stiffeners at the same X position, due to friction. The velocities of

the tracing points at the middle of the plate along the exit of the extrusion die are shown in Fig. 5c. It is obvious that the velocity increases gradually from the end to the middle of the plate in design 1, while the velocity distribution of design 2 is much uniform. The maximum velocity difference of design 1 is 0.21 mm/s, 10 times larger than that of design 2 (0.02 mm/s). The standard deviation of the velocity (SDV) is introduced in this study to quantitatively evaluate the velocity distribution, which is described as

$$SDV = \sqrt{\frac{\sum_{i=1}^n (v_i - \bar{v})^2}{N}} \quad (2)$$

where N is the total number of the selected points, v_i is the axial velocity at point i , and \bar{v} is the average velocity for all selected points. SDV values of the two designs and design 2 with different extrusion speeds are shown in Fig. 5d. It can be seen that the SDV of design 1 is 10 times larger than that of design 2 at the same extrusion speed, and the SDV values increase slightly with decreasing extrusion speed in design 2. This result is consistent with the research of Zhang et al. [26], which showed that more uniform velocity distribution in the cross-section of the extrudate can be achieved by a larger extrusion speed. When the extrusion speed is decreased, the extruded material spends more time in the extrusion process, which can lead to variations in the flow rate and therefore result in an increase in the SDV value.

Fig. 5 a–d The velocity along die exits and SDV values for the two extrusion die designs with the same extrusion speed of 2 mm/s



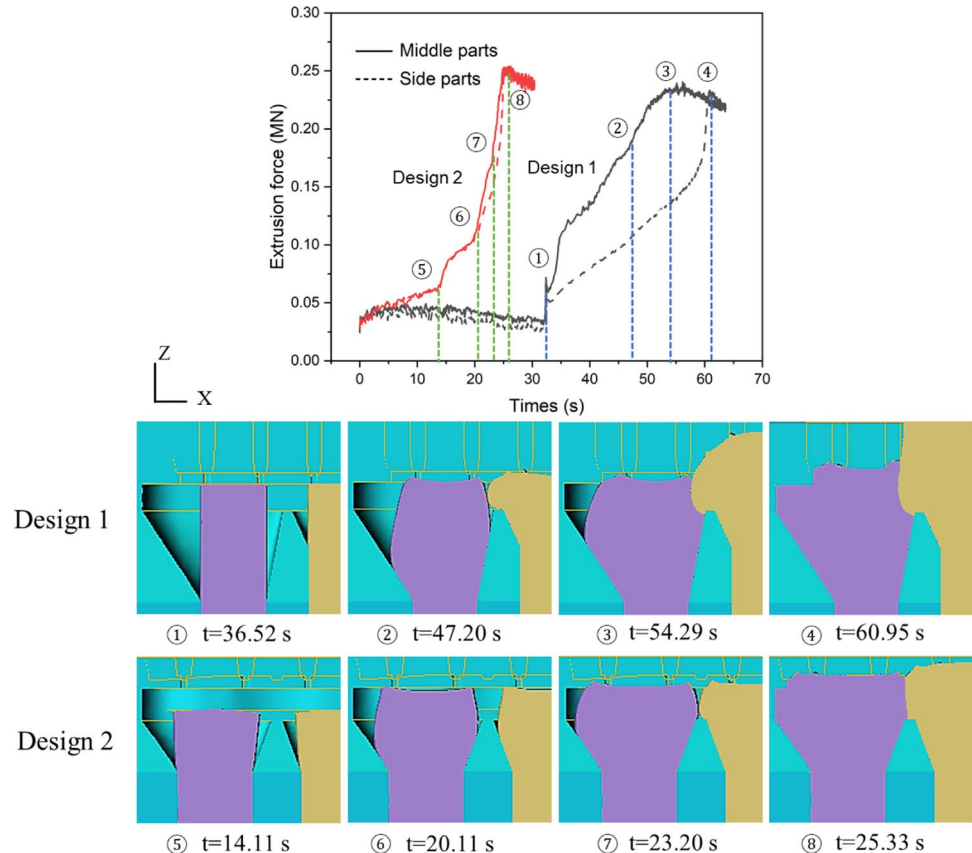
4.2 Extrusion force

Extrusion force is an important evaluation index for the design of extrusion dies and also helps to fully understand the metal flow behaviour. Figure 6 presents the extrusion force of the multi-container extrusion with different die designs and the metal flow patterns in different extrusion stages. As shown in Fig. 6, the highest extrusion forces of the middle and side parts of the initial design and modified design are similar, around 0.25 MN and 0.24 MN, respectively, while two designs have different trends of extrusion force curves. The total extrusion forces (sum of three containers) of design 1 and design 2 of the multi-container extrusion are 0.68 MN and 0.76 MN respectively. Compared with design 1, the extrusion force of design 2 is slightly higher due to the increased friction caused by the upper die channels and the second-step welding chamber.

For design 1, its stepped rise shows a three-stage process. The extrusion force of the first stage is around 0.04 MN before time (1), which indicates in this stage that billets are mainly affected by friction and they have not been plastically deformed until they reach the wall of the welding chamber. In the second stage, all billets start spreading to fill the channels and the welding chamber. The metal flows start to meet each other at time (2). During this spreading process, the

volume that needs to be filled in the sides is much larger than that in the middle, resulting in a large difference in extrusion forces. The extrusion force in the middle part is mainly used for extruding the middle billet out of the die bearing, while the extrusion forces in both side parts are mainly applied for the expansion of the side billets. This leads to such a large difference in extrusion forces and thus results in the uneven metal flow in design 1. Besides, the metal in the middle part would flow to both sides preferentially compared to the outflow, so that the position of the weld line is biased to the side parts rather than between the two containers. This also results in the front end of the middle part of the extrudate being longer than that of both sides (Fig. 4). At time (3), the extrusion force of the middle part reaches the peak value but that of the side parts starts to increase rapidly because it is still in the spreading process. It is not until time (4) that the welding chamber is completely filled, and at the same time, the extrusion force on side parts reaches the peak value. In the third stage, the extrusion load gradually decreases with further extrusion as billet length and total friction force decrease. As for design 2, there are four stages. The difference of extrusion forces in the middle part and side parts is much smaller than that of design 1, which indicates that design 2 has a better metal flow uniformity. Unlike design 1, in the first stage, the extrusion force increases slightly before

Fig. 6 Predicted extrusion forces of design 1 and design 2 at an extrusion speed of 2 mm/s and forming stages in multi-container extrusion



time (5), showing that the billets begin to plastically deform and spread as soon as they enter the channels. After they touch the wall of the first-step welding chamber and start to enter the second-step welding chamber, the extrusion force increases rapidly, which is the second stage, as shown from time (5) to time (6) in Fig. 6. During the third stage which is to fill the welding chamber stage, the metal flows begin to weld at time (7). The extrusion forces reach a peak after the metal flows fill the welding chamber, as shown at time (8). The last stage in design 2 is the same as that in design 1, which presents the stable extrusion process.

4.3 Welding quality analysis

During the multi-container extrusion process, welding mainly occurs at gap positions between containers in the welding chamber. The schematic diagram of the welding process is shown in Fig. 7. Two metal flows from the adjacent extrusion containers after the expansion process meet in the welding chamber and then would be welded and finally extruded to obtain a wide profile. When the separated metal

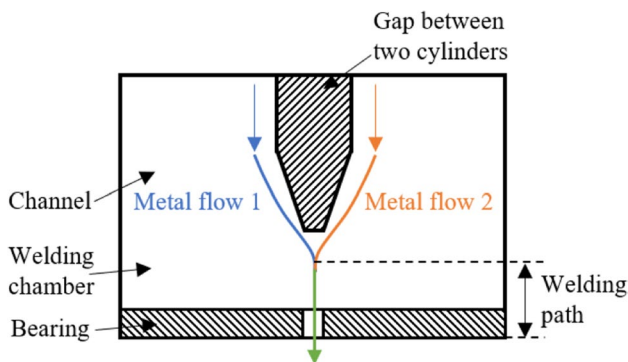
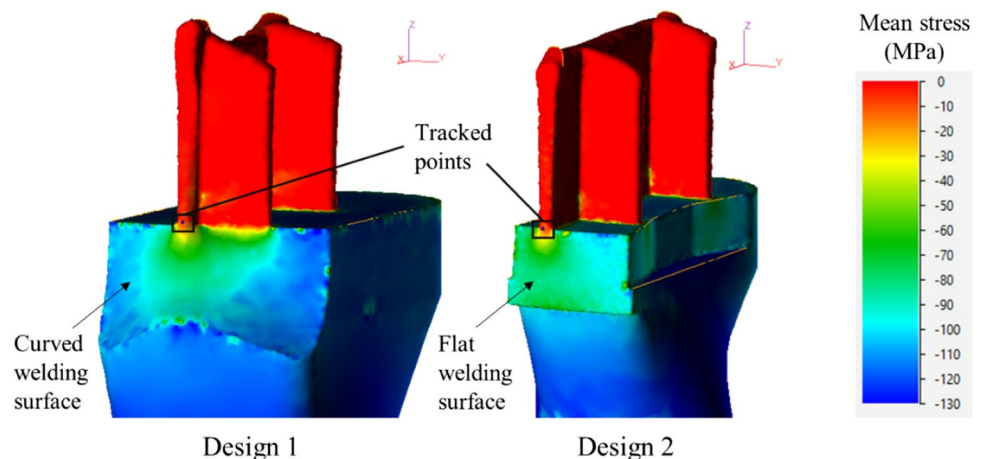


Fig. 7 Schematic diagram of welding path in multi-container extrusion process

Fig. 8 Mean stress distribution and the tracked points for analysis of predicted welding quality in design 1 and design 2



flows contact each other in the welding chamber, solid-state bonding proceeds along the welding line, and the atoms on the surface of metal flows gradually approach each other under the action of plastic deformation and atomic diffusion, forming intimate micro-level contacts [27].

In the multi-container extrusion, the welding quality of the product is one of the most important factors to evaluate the extrusion die design. In the QForm software, the pressure p has the same absolute value as the mean stress σ_m , but they are opposite in sign. Figure 8 shows the mean stress distribution on the welding plane between two billets. There is a curved surface of the welding area in design 1, while the welding plane in design 2 is a flat surface. The distribution of the mean stress σ_m near the outlet is similar in both designs. The tracked points used for welding quality assessment are chosen in the middle of the welding plane of the base plate as shown in Fig. 8.

Figure 9a shows the movement of the tracked points in design 1 and design 2 at different extrusion times, from which the welding time can be obtained in Fig. 9b. The welding time is defined as the period from the moment two metal streams meet to the moment they flow out of the die. If the welding time is short, the material may not be sufficiently welded, leading to defects. As shown in Fig. 9b, the welding times of the tracked points for the initial die design and modified die design at an extrusion speed of 2 mm/s are 16.15 s and 6.68 s, respectively. The reason for the difference in the welding time is that the length of the welding path is different. For design 1, it is not straight and is longer than that of design 2, as shown in Fig. 9a. The speed of the tracking point in the Z-direction of the initial design is slow in the early stages of welding since it travels horizontally instead of vertically, which results in the welding time of the initial die design being longer.

Figure 10 shows the changes of some parameters related to the welding quality for different extrusion die designs during the extrusion process. Figure 10a shows pressure

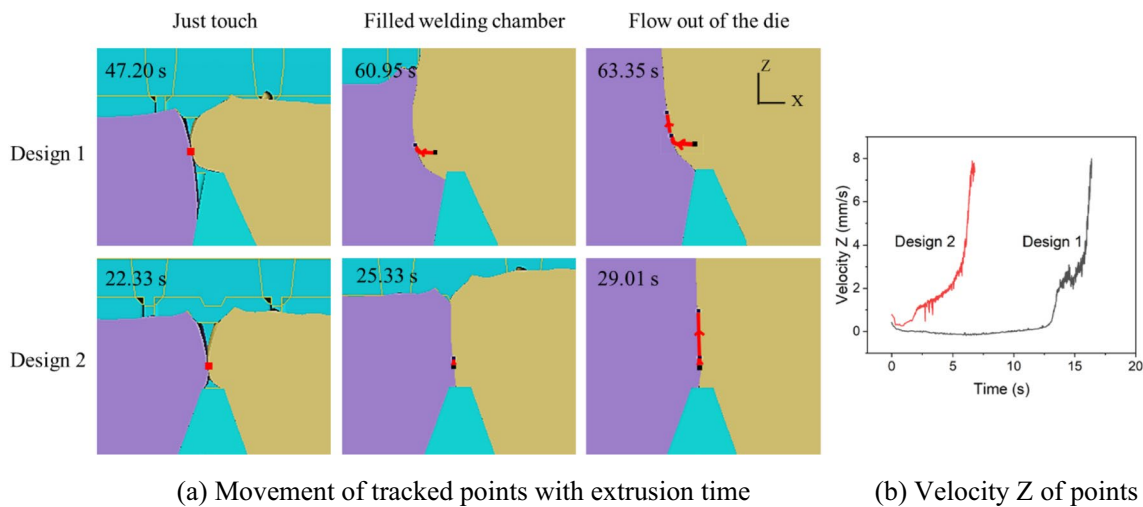


Fig. 9 a, b Movement and velocity Z of tracked points in welding path of design 1 and design 2

changes of the tracing points during welding. For design 1, after two metal flows contact each other, with the increase of the welding time, the pressure increases rapidly to about 30 MPa and then increases slowly to about 60 MPa until the welding time of 12.5 s, followed by a rapid increase to the peak value (around 85 MPa) and finally decrease to 0 MPa. The trends of the pressure for design 2 are different with that of design 1 at the same extrusion speed. The pressure curve of design 2 increases first and then decreases with a peak value of 90 MPa. With the decrease of extrusion speed, the peak of pressure gradually reduces. Figure 10b shows the effective stress of the tracing points during welding. The effective stress in design 1 has a fluctuating trend in the early stage of welding and then increases rapidly to the peak value (31.2 MPa), while the effective stress in design 2 remains stable firstly and then increases to the peak value (30.0 MPa). With the reduction of the extrusion speed, the peak of effective stress gradually drops. The ratio of pressure to effective stress is shown in Fig. 10c, the maximum values for design 1 and design 2 all reach 3–4, so the welding quality could be ensured in this study according to the welding criterion of Donati and Tomesani [28]. This will be detailed later in this section. In addition, the peak values of the ratio for design 2 at different extrusion speeds are not much different but higher than that of design 1. Figure 10d shows the strain rate of the tracing points during the welding process. All strain rates for designs at different extrusion speeds are almost 0 s^{-1} at the early stage of welding and then increase rapidly. The strain rate of design 1 has the highest peak value, and the peak value of design 2 decreases gradually as the extrusion speed reduces. Figure 10e shows the temperature of design 2 at different extrusion speeds. It is obvious that the temperature reduces with the decrease in the extrusion speeds.

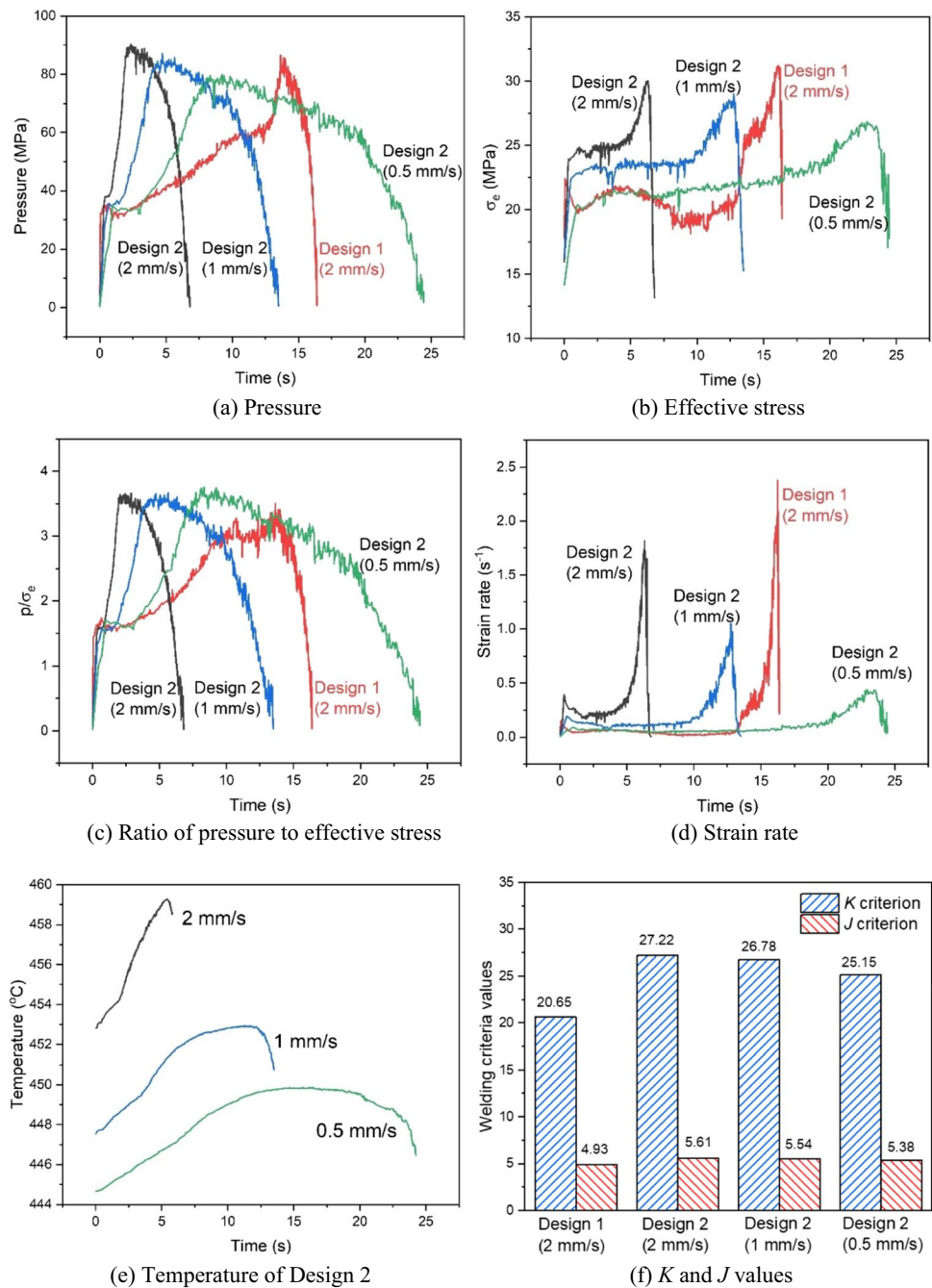
Several criteria have been proposed to evaluate extrusion welding quality by means of a large number of experiments, such as the maximum pressure criterion (*P* criterion) [29], pressure–time criterion (*Q* criterion) [30], pressure–time–flow criterion (*K* criterion) [31], and dimensionless solid-state bonding criterion (*J* criterion) [32]. *P* criterion only considers the influence of internal pressure on welding quality, regardless of other factors such as stress, contacting time, and dead metal zone (DMZ). *Q* criterion also ignores the effect of DMZ. Since the two designs in this study have much difference in the dead metal zone, the *P* and *Q* criteria are not accurate assessments of the welding quality. Therefore, the *K* and *J* criteria were used to evaluate the welding quality of the two designs.

K criterion is based on the integral in the welding path of the ratio of welding pressure *p* to effective stress σ_e of the material.

$$K = \int_0^t \frac{p}{\sigma_e} dt \cdot v = \int_0^L \frac{p}{\sigma_e} dl \geq \text{Const.} \tag{3}$$

where *t* is the contact time (s), *v* is the metal flow velocity (mm/s), and *L* (mm) is the welding path from the endpoint of the die bridge up to the die exit, where pressures are zero. Const. is the weld limit, representing a threshold value to determine if the extrusion welding would take place. This value varies with different combinations of the process parameters including temperature, extrusion ratio, and ram speed, as well as the material properties such as flow stress and chemical composition. For a given material under specific forming conditions, the value is a constant. The investigation of Donati and Tomesani [28] showed that once the ratio of the pressure to flow stress approximately reached 3 or 4, the welding quality during an extrusion could be ensured.

Fig. 10 a–f Pressure, effective stress, the ratio of pressure to effective stress, strain rate, temperature, and K and J values of design 1 and design 2



J criterion was proposed by Yu et al. [32] considering the process of void closure and sound bonding formation:

$$J = \int_0^t k_0 \frac{\sigma_m \dot{\varepsilon}}{\sigma_e} \exp\left(\frac{RT}{Q_D}\right) dt \quad (4)$$

where k_0 is a coefficient related to material and the surface conditions of metal for bonding, σ_m is the mean normal stress, $\dot{\varepsilon}$ is the effective strain rate (s^{-1}), R is the universal gas constant ($8.314 \text{ J/mol} \cdot \text{K}$), T is the absolute temperature (K), and Q_D is the diffusion activation energy (J/mol), which is

$1.42 \times 10^5 \text{ J/mol}$ for self-diffusion of aluminium atoms at the temperature range of $450\text{--}650 \text{ }^\circ\text{C}$. The ratio of pressure to effective stress and effective strain in the region surrounding the voids is the main factor in the void closure behaviour [33].

Figure 10f shows the results calculated according to the K and J criteria using the data shown in Fig. 10a–e. Researchers [32, 34] calculated the K or J values by using tracked points to obtain the pressure, effective stress, and effective strain rate in different positions on the welding plane to compare welding quality. Therefore, the same method is used to compare the welding quality of the two designs. For the K criterion, it

is noted that the value of design 2 (27.22) is larger than that of design 1 (20.65) at the same extrusion speed. Besides, with the decrease in the extrusion speed, the values of the K criterion drop slightly. For the J criterion, the value of design 2 (5.61) is also higher than that of design 1 (4.93) at an extrusion speed of 2 mm/s, and it reduces slightly with decreasing extrusion speeds. Therefore, the welding quality of design 2 is better than that of design 1. In addition, extrusion speed will affect the increment of billet's temperature and the distribution of pressure in the welding chamber [35]. Higher billet temperature is beneficial to reduce flow stress, which makes metal flows easier to deform and weld. The pressure and the temperature increase when the extrusion speed increases in design 2 (Fig. 10a, e), leading to the increase in the welding quality in this study. But if the speed is too fast, the material may not have enough time to weld properly, resulting in weak or incomplete welds. Hence, appropriate extrusion speed is needed to ensure the good welding quality.

4.4 Die deflection

Extrusion dies usually work under high temperature, pressure, and friction environment, and die plastic deformation and cracking might occur, which could affect the accuracy of extruded profiles and the die service life [36]. Due to the modified extrusion die design in this study which has a reduced thickness for the upper die and the lower die, it is necessary to compare its die deformation with that of the initial die.

Figure 11 shows the effective stress, effective strain, and X-axial displacement distribution in design 1 and design 2. The maximum effective stress, effective strain, and X-axial displacement for design 1 are 320 MPa and 0.0016 and 0.025 mm, while these for design 2 are 240 MPa and 0.0012 and 0.017 mm. The locations of the maximum value for different designs are all at the entrance of the channels. This indicates the structure of design 2 has a smaller maximum effective stress and effective strain. The maximum effective stress of two designs is less than the yield stress of H13, which is about 1100 MPa at 500 °C. The maximum effective strains occurred out of the die bearing for the lower dies in this study, because the boundary condition is set to fix the bottom of the lower die and the bottom of the bearing is a stepped structure where stress concentration occurs. Besides, the maximum X-axial displacements in the outlet of the lower die for design 1 and design 2 are 0.006 and 0.003 mm respectively, which has little effect on the shape deflection of the final profile.

4.5 Comparison among traditional and multi-container extrusions

To produce the same dimension of the extrudate, the diameter of the traditional extrusion container/billet should

be more than the width of the stiffened panel (177 mm). The dimensions of billets used for the traditional extrusion and both designs of the multi-container extrusion are $\Phi 200 \times 1000$ mm (the ratio of length to diameter of the billet is typically 5:1 [37]) and $\Phi 37 \times 185$ mm respectively. Table 1 shows the comparison of maximum extrusion force in the traditional extrusion and the multi-container extrusion. The extrusion force (F) in the traditional extrusion is estimated as [38]:

$$F = P \times A \quad (5)$$

$$P = \bar{\sigma}(a + b \ln \lambda + c L_B) \quad (6)$$

where P is the pressure, $A = 3.14 \times 10^4 \text{ mm}^2$ is the area of the billets, $\bar{\sigma} = 8.37 \text{ MPa}$ is the mean equivalent flow stress, $\lambda = 44.19$ is the extrusion ratio, $L_B = 1000 \text{ mm}$ is the length of the billet, a is the coefficient which represents the contribution of the massive redundant work associated with this form of deformation, b is an indication that deformation is far from the homogenous event, and c is the friction coefficient. The extrusion force of the traditional extrusion is calculated to be 6.60 MN, while the total extrusion forces of design 1 and design 2 of the multi-container extrusion are simulated by QForm to be only 0.68 MN and 0.76 MN respectively, which are about one-tenth of the traditional extrusion force. The main reason is that the multi-container extrusion greatly reduces the extrusion ratio and thus reduces the extrusion forces.

In the initial extrusion die design, a great deal of material would be wasted, so saving material in the multi-container extrusion has been an important issue. Table 1 also shows the volume of material waste in different extrusion processes. The material trapped in the die of design 2 is normalised by the values of design 1 to compare the two designs. Generally, the material yield, defined as a ratio of total product weight to total billet weight, is about 85% in the conventional extrusion of aluminium profiles [39]; thus, the material waste in the traditional extrusion is calculated as 15% of the billet volume. Assuming the material waste in the multi-container extrusion is mainly in the channels and the welding chamber, the material waste volume (material trapped in die) could be obtained by calculating the sum of the volume of channels and the welding chamber, as shown in Table 1. The proportion of material waste to the overall billet material in the multi-container extrusion is calculated to be 69.5% and 30.0%, respectively, for design 1 and design 2. It should be noted that the proportion of wasted material to the overall billet of the multi-container extrusion is higher than that of the traditional extrusion, since the diameter and length of the billets will be reduced (the ratio of length to the diameter of the billet is typically 5:1 [37]). The billet material in design 1 is wasted seriously, while design 2 could

Fig. 11 Effective stress, effective strain, and displacement X of extrusion die during stable extrusion process of design 1 and design 2

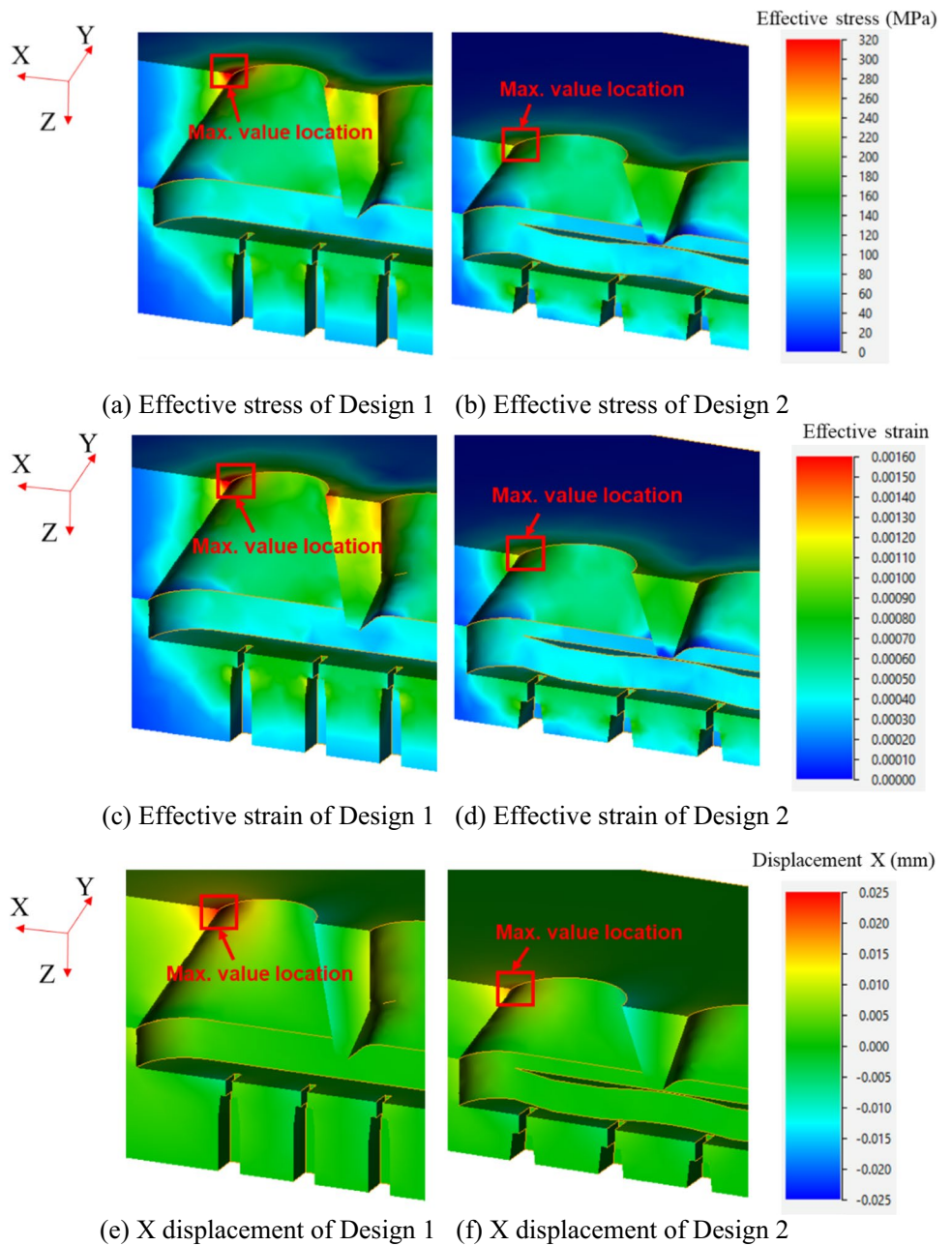


Table 1 Comparison of predicted extrusion forces at an extrusion speed of 2 mm/s and material trapped in the die (waste) among the traditional extrusion and the two designs of multi-container extrusions

	Traditional extrusion	Design 1 of multi-container extrusion	Design 2 of multi-container extrusion
Extrusion ratio	44.19	4.54	4.54
Extrusion force (MN)	6.60	0.68	0.76
Total billet volume (mm ³)	3.14 × 10 ⁷	5.97 × 10 ⁵	5.97 × 10 ⁵
Material trapped in die (mm ³)	4.71 × 10 ⁶	4.15 × 10 ⁵	1.79 × 10 ⁵
Normalised extrusion force	1.0	0.103	0.115
Normalised material trapped*	–	1.0	0.431

*Normalised by the value of design 1

save 39.5% of material compared to design 1, which means that the modified die design can greatly increase the material utilisation in the multi-container extrusion. Although the proportion of material waste to the overall billet material in the multi-container extrusion is higher than the generally acknowledged 15% in the traditional extrusion, the advantage of extrusion force saving is particularly significant.

5 Conclusions

The multi-container extrusion will be a trend for the production of wide profile due to the low extrusion force, which can significantly save energy and reduce CO₂ emission. It is meaningful to systematically study its mechanism and optimise the die designs to improve the quality of the extrudates. This paper optimises the dies of the multi-container extrusion by using the FE method, and the feasibility of the new design for this novel extrusion technology will be experimentally investigated in the future research. In the present work, modified extrusion dies were designed for the multi-container extrusion in order to reduce material waste and improve the metal flow uniformity and welding quality. The extrusion processes using the initial dies and the modified dies for wide stiffened aluminium panels were investigated numerically. The effect of the modified die design on the material flow behaviour, extrusion forces, welding qualities, die deflection, and material utilisation was synthetically studied and compared with the initial die design by analysing the simulated results. Besides, the effect of extrusion speed on the extrusion process was evaluated by using the modified design. The extrusion force and material utilisation of the multi-container extrusion and the traditional extrusion were compared. The main findings in this study are summarised as follows:

1. A more uniform velocity distribution on the cross-section of the die exit in the modified extrusion dies (design 2) is obtained, and the front-end shape is better than that obtained with the initial dies (design 1). The SDV of velocity for the modified design is 10% that of the initial design for the same extrusion speed, and decreasing the extrusion speed only slightly increases the SDV values for the modified design.
2. The total extrusion forces of the 3-container extrusion system are about one-tenth of the traditional extrusion for producing wide stiffened aluminium panels. The extrusion force of design 2 (0.76 MN) is slightly higher than that of design 1 (0.68 MN) due to the increased friction, and the extrusion force of each container (side parts and middle part) of design 2 is relatively uniform while that of the initial die design varies greatly.

3. The welding quality of design 2 is better than that of design 1. The values of K (27.22) in design 2 are higher than K (20.65) in design 1 at the same extrusion speed of 2 mm/s, and J (5.61) in design 2 is greater than J (4.93) in design 1. With the decrease of the extrusion speed from 2 mm/s to 0.5 mm/s, the value of the K criterion for the modified die design drops slightly from 27.22 to 25.15, while the value of the J criterion drops slightly as well, from 5.61 to 5.38.
4. The modified die design can effectively increase the material utilisation rate for the multi-container extrusion, which can save 39.5% material compared to the initial die design.

Author contribution Zhe Zhang: data curation, methodology, investigation, visualisation, and writing (first draft of the manuscript). Wenbin Zhou: methodology, investigation, supervision, and writing (reviewing and editing). Zhusheng Shi: conceptualization, project administration, supervision, and writing (reviewing and editing). Jianguo Lin: conceptualization, funding acquisition, supervision, and writing (reviewing and editing).

Funding This work was supported by EPSRC under the Grant Agreement EP/R001715/1 on “LightForm: Embedding Materials Engineering in Manufacturing with Light Alloys” and EP/S019111/1 on “UK-FIRES: Locating climate mitigation at the heart of industrial strategy”. Z. Zhang has received research support from China Scholarship Council.

Data availability The datasets used or analysed during the current study are available from the corresponding author on reasonable request.

Code availability Not applicable.

Declarations

Ethics approval Not applicable.

Consent to participate Not applicable.

Consent for publication Yes.

Competing interests The authors declare no competing interests.

Open Access This article is licensed under a Creative Commons Attribution 4.0 International License, which permits use, sharing, adaptation, distribution and reproduction in any medium or format, as long as you give appropriate credit to the original author(s) and the source, provide a link to the Creative Commons licence, and indicate if changes were made. The images or other third party material in this article are included in the article's Creative Commons licence, unless indicated otherwise in a credit line to the material. If material is not included in the article's Creative Commons licence and your intended use is not permitted by statutory regulation or exceeds the permitted use, you will need to obtain permission directly from the copyright holder. To view a copy of this licence, visit <http://creativecommons.org/licenses/by/4.0/>.

References

- Joost WJ (2012) Reducing vehicle weight and improving US energy efficiency using integrated computational materials engineering. *JOM* 64:1032–1038
- Zhang Z, Zhou W, Shi Z, Lin J (2022) Advances on manufacture methods for wide lightweight aluminium stiffened panels. *IOP Conf Ser: Mater Sci Eng* 1270:012122
- Yoon JW, Bray G, Valente R, Childs T (2009) Buckling analysis for an integrally stiffened panel structure with a friction stir weld. *Thin Wall Struct* 47:1608–1622
- Harris DK, Gheitis A (2013) Implementation of an energy-based stiffened plate formulation for lateral load distribution characteristics of girder-type bridges. *Eng Struct* 54:168–179
- Lynch C, Murphy A, Price M, Gibson A (2004) The computational post buckling analysis of fuselage stiffened panels loaded in compression. *Thin Wall Struct* 42:1445–1464
- Liu H, Lei Z, Jiang H, Zou J, Guo Z, Bai R, Wang D (2022) Study on shear buckling failure of laser-welded dissimilar aluminum alloy (Al-Li-2099/Al-Li-S4) stiffened panel. *J Laser Appl* 34:022012
- Li B, Gao H, Deng H, Wang C (2020) A machining deformation control method of thin-walled part based on enhancing the equivalent bending stiffness. *Int J Adv Manuf Technol* 108:2775–2790
- Liu B, Doan VT, Garbatov Y, Wu W, Guedes Soares C (2020) Study on ultimate compressive strength of aluminium-alloy plates and stiffened panels. *J Mar Sci Appl* 19:534–552
- Jingan L (2001) Production process and key technology of a large industries aluminium alloy extruded shapes. *Aluminium Fabr* 2:191–199
- Wang D, Zhang C, Wang C, Zhao G, Chen L, Sun W (2018) Application and analysis of spread die and flat container in the extrusion of a large-size, hollow, and flat-wide aluminum alloy profile. *Int J Adv Manuf Technol* 94:4247–4263
- Liu Z, Li L, Yi J, Wang G (2019) Entrance shape design of spread extrusion die for large-scale aluminum panel. *Int J Adv Manuf Technol* 101:1725–1740
- Aalberg A, Langseth M, Larsen P (2001) Stiffened aluminium panels subjected to axial compression. *Thin Wall Struct* 39:861–885
- Valente R, Yoon R, Bray G, Childs T (2010) On the influence of FSW in the elastoplastic buckling load-carrying capacity of extruded integrally stiffened panels for aeronautic applications. *Int J Mater Form* 3:1019–1022
- Munroe J, Wilkins K, Gruber M (2000) Integral Airframe Structures (IAS): validated feasibility study of integrally stiffened metallic fuselage panels for reducing manufacturing costs. *NASA/CR-2000-20933* 133–135
- Lv J, Yu J, Shi Z, Li W, Lin J (2023) Feasibility study of a novel multi-container extrusion method for manufacturing wide aluminium profiles with low force. *J Manuf Process* 85:584–593
- Li W, Yu J, Lv J, Shi Z, Lin J (2022) Development of a multi-container extrusion method for extruding lightweight wide plates and sheets. *IOP Conf Ser: Mater Sci Eng* 1270:012061
- Dong Y, Zhang C, Luo W, Yang S, Zhao G (2016) Material flow analysis and extrusion die modifications for an irregular and multitooth aluminum alloy radiator. *Int J Adv Manuf Technol* 85:1927–1935
- Elgeti S, Probst M, Windeck C, Behr M, Michaeli W, Hopmann C (2012) Numerical shape optimization as an approach to extrusion die design. *Finite Elem Anal Des* 61:35–43
- Lee GA, Kwak DY, Kim SY, Im YT (2002) Analysis and design of flat-die hot extrusion process 1. Three-dimensional finite element analysis. *Int J Mech Sci* 44:915–934
- Lee GA, Im YT (2002) Analysis and die design of flat-die hot extrusion process 2. Numerical design of bearing lengths. *Int J Mech Sci* 44:935–946
- Zhou W, Yu J, Lu X, Lin J, Dean TA (2021) A comparative study on deformation mechanisms, microstructures and mechanical properties of wide thin-ribbed sections formed by sideways and forward extrusion. *Int J Mach Tool Manuf* 168:103771
- Chen L, Zhao G, Yu J, Zhang W, Wu T (2014) Analysis and porthole die design for a multi-hole extrusion process of a hollow, thin-walled aluminum profile. *Int J Adv Manuf Technol* 74:383–392
- Liu P, Xie S, Cheng L (2012) Die structure optimization for a large, multi-cavity aluminum profile using numerical simulation and experiments. *Mater Des* 36:152–160
- Sun X, Zhao G, Zhang C, Guan Y, Gao A (2013) Optimal design of second-step welding chamber for a condenser tube extrusion die based on the response surface method and the genetic algorithm. *Mater Manuf Processes* 28:823–834
- Biba N, Stebunov S, Vlasov A (2017) Material forming simulation environment based on QForm3D software system. *12th Int Conf Metal Form* 2:4
- Zhang C, Zhao G, Chen H, Guan Y, Li H (2012) Optimization of an aluminum profile extrusion process based on Taguchi's method with S/N analysis. *Int J Adv Manuf Technol* 60:589–599
- Cooper DR, Allwood JM (2014) Influence of diffusion mechanisms in aluminium solid-state welding processes. *Procedia Manuf* 81:2147–2152
- Donati L, Tomesani L (2005) The effect of die design on the production and seam weld quality of extruded aluminum profiles. *J Mater Process Technol* 164:1025–1031
- Akeret R (1972) Properties of pressure welds in extruded aluminium alloy sections. *J Inst Met* 10:202–210
- Plata M, Piwnik J (2000) Theoretical and experimental analysis of seam weld formation in hot extrusion of aluminum alloys. *Proceedings of the 7th international aluminum extrusion technology seminar*, vol 1. Chicago, pp 205–211
- Donati L, Tomesani L (2004) The prediction of seam welds quality in aluminum extrusion. *J Mater Process Technol* 153:366–373
- Yu J, Zhao G, Chen L (2016) Analysis of longitudinal weld seam defects and investigation of solid-state bonding criteria in porthole die extrusion process of aluminum alloy profiles. *J Mater Process Technol* 237:31–47
- Nakasaki M, Takasu I, Utsunomiya H (2006) Application of hydrostatic integration parameter for free-forging and rolling. *J Mater Process Technol* 177:521–524
- Yu J, Zhao G, Cui W, Chen L, Chen X (2019) Evaluating the welding quality of longitudinal welds in a hollow profile manufactured by porthole die extrusion: experiments and simulation. *J Manuf Process* 38:502–515
- Lu X, Zhang C, Zhao G, Guan Y, Chen L, Gao A (2016) State-of-the-art of extrusion welding and proposal of a method to evaluate quantitatively welding quality during three-dimensional extrusion process. *Mater Des* 89:737–748
- Giarmas E, Tzetzis D (2022) Optimization of die design for extrusion of 6xxx series aluminum alloys through finite element analysis: a critical review. *Int J Adv Manuf Technol* 119:5529–5551
- Chien K, Robbins P, Jowett C, Wang Y (2018) Extrusion productivity, Part I – billet geometry. *Light Metal Age*, pp 28–31
- Sheppard T (1999) Extrusion of aluminium alloys. *Bournemouth University, Springer Science & Business Media*
- Hassamontr J, Leephaicharoen T (2020) Modeling of aluminum profile extrusion yield: pre-cut billet sizes. *Int Conf Intell Comput Optim* 1324:452–462

Publisher's note Springer Nature remains neutral with regard to jurisdictional claims in published maps and institutional affiliations.